dissociation energies when modeled by statistical phase-space theory.

Acknowledgment. We thank the National Science Foundation for supporting this research through Grants CHE87-11567 (J.L.B.) and CHE88-17201 (M.T.B.). We are also grateful to the Shell Foundation for graduate fellowship funding (D.V.D.) and to the donors of the Petroleum Research Fund, administered by the American Chemical Society, for additional support. We also thank Denley Jacobson for taking some of the original data.

Appendix

Calculation of kinetic energy release distributions, with use of phase-space theory to model the decomposition of metastable ions, requires a number of input parameters. The calculations are fairly insensitive to the parameters listed in Table II, including rotational constants B, symmetry parameters σ, neutral polarizabilities α, and vibrational frequencies ν_i. Values of B were taken from the literature where available[34] or calculated from typical Fe^+–C, C–C, and C–H bond lengths. Polarizabilities were estimated with the atomic hybrid components method.[35] Vibrational frequencies were taken from literature[36] where possible or estimated from literature values of similar species. The estimated frequencies were varied over the entire physically reasonable range for these quantities and were found not to affect the details of the kinetic energy release distributions over this range.

The phase-space calculations are quite sensitive to the total energy available for partitioning among the various modes and, hence, to the heats of formation of the reactants and products. The values employed are listed in Table III. As noted in the Results and Discussion, in cases where the heats of formation of all reactants and products save one are known, the remaining heat of formation can be determined by varying it as a free parameter to achieve a fit of the calculated results to the experimental measurements. This method was used to obtain the values for the organometallic ions reported in Table III.

(34) Landolt-Bornstein, H. H. *Numerical Data and Functional Relationships in Science and Technology, New Series, Group II*; Hellwege, K. H., Hellwege, A. M., Eds.; Springer-Verlag: Berlin, 1974, 1976; Vols. 6, 7.

(35) Miller, K. J.; Savchik, J. A. *J. Am. Chem. Soc.* **1979**, *101*, 7206-7213.

(36) (a) Shimanouchi, T. *Table of Molecular Vibrational Frequencies*; National Bureau of Standards: Washington, DC, 1972; Consolidated Vol. 1. (b) Sverdlov, L. M.; Kovner, M. A.; Krainov, E. P. *Vibrational Spectra of Polyatomic Molecules*; Wiley: New York, 1970.

Comparative Study of Resonance Raman and Surface-Enhanced Resonance Raman Chlorophyll *a* Spectra Using Soret and Red Excitation

Lana L. Thomas, Jae-Ho Kim, and Therese M. Cotton*

Contribution from the Department of Chemistry and Ames Laboratory, Iowa State University, Ames, Iowa 50011. *Received April 9, 1990. Revised Manuscript Received August 3, 1990*

Abstract: Surface-enhanced resonance Raman scattering (SERRS) spectra are reported for chlorophyll *a* adsorbed on a silver electrode at 298 and 77 K with 406.7-, 457.9-, 514.5-, and 647.1-nm excitation. Submerging the electrode in degassed water at 298 K was found to improve the spectral quality by minimizing sample heating and photooxidation. Spectral intensities and peak resolutions were greater at all excitation wavelengths at liquid nitrogen temperature. Most significantly, roughened silver at the low temperature quenched the fluorescence accompanying red excitation and minimized sample photooxidation, resulting in richly detailed SERRS spectra of chlorophyll *a*. The close correspondence between chlorophyll *a* resonance Raman (RR) and SERRS spectra suggests that an electromagnetic mechanism is the major source of the surface enhancement, rather than a chemical mechanism (e.g. a charge-transfer complex between chlorophyll *a* and the metal). The spectral similarities, together with the presence of the MgN_4 vibration band in the SERRS spectra, also provide evidence that structural alterations (e.g. cleavage of ring V or loss of Mg) do not occur in chlorophyll *a* after adsorption at the electrode surface. A distinctive SERRS spectrum was obtained for each excitation wavelength. Selective excitation within the various electronic transitions can thus be utilized to verify assignments of the vibrational modes of chlorophyll *a* and to monitor its interactions and photochemical behavior in biomimetic systems.

Introduction

Chlorophyll *a* (Chl *a*) plays an essential role in the conversion of sunlight into chemical energy in green plants and blue green algae. Chlorophylls are metallochlorins (dihydrogen-reduced metalloporphyrins) found in photosynthetic membranes. The obligatory presence of metalochllorins in lieu of metalloporphyrins in photosynthetic and certain other biological systems is not understood. However, in an attempt to elucidate the structural and photochemical behavior of these compounds, resonance Raman (RR) spectroscopy has been utilized as a probe of the vibrational and electronic structure of metalloporphyrins[1-4] and, more recently, metallochlorins and chlorophylls.[5-12] The latter species result from reduction of the $C_b{=}C_b$ bond of ring IV of the porphyrin macrocycle. This destroys the in-plane degeneracy and has a profound effect on the electronic absorption spectrum. The typical B and Q electronic transitions of symmetrical porphyrins are split into x and y components. In addition, the Q transition gains considerable intensity relative to that observed in porphyrins.

The differences in the chlorin electronic properties are reflected in their RR spectra, which are strongly affected by excitation conditions. Resonance Raman excitation within the strongly allowed B transition results in enhancement of symmetric, in-plane modes arising primarily from Franck-Condon type scatter-

* Author to whom correspondence should be addressed.

(1) Johnson, B. B.; Peticolas, W. *Annu. Rev. Phys. Chem.* **1976**, *27*, 465-491.

(2) Spiro, T. G.; Stein, P. *Annu. Rev. Phys. Chem.* **1977**, *28*, 501-521.

(3) Felton, R. H.; Yu, N.-T. In *The Porphyrins*; Dolphin, D., Ed.; Academic Press: New York, 1978; Vol. II, pp 341-388.

(4) Spiro, T. G. In *Iron Porphyrins*; Lever, A. B. P., Gray, H. B., Eds.; Addison-Wesley: Reading, MA, 1982; Part II, pp 89-152.

0002-7863/90/1512-9378$02.50/0

ing[9a,10a,d,e,11,13b], although a small contribution from non-Condon mechanisms has been estimated recently.[14] Excitation within the Q_x band produces enhancement via vibronic coupling between this state and the intense B state(s). Excitation within the Q_{y0} transition has been accomplished in only a few instances by using various subterfuges to avoid or reduce the intense fluorescence from this state.[7b,c,12,14] For example, Koningstein et al.[14] have recently obtained resonance excitation profiles for two modes in Ni Pheo *a* within the Q_y 0,0 and 0,1 region of the absorption spectrum. Their results indicate significant (ca. 40%) non-Condon activity within this excitation region as a result of vibronic coupling to one or more of the B states. Thus, the RR scattering mechanisms within this transition appear to be much more complex than in the case of porphyrins of higher symmetry.

Several investigations have focused on Raman spectroscopy of isolated chlorophyll pigments as a first step in understanding their role in the photosynthetic membrane.[10a,b,9,11,15] RR band assignments have been suggested for a number of chlorophylls.[10] The objective of the RR investigations of chlorophyll *a* has been to define the effect of axial coordination[16] on the RR (as well as IR) spectra,[9a] to identify bands that are both ligation and metal sensitive,[9,15] and to determine the effects of isotopic substitution on the spectrum in an effort to assign bands to specific vibrations of the macrocycle.[17] Both RR[11] and FTIR difference spectroscopy[18] have also been used to characterize the Chl *a* cation radical vibrational spectrum.

In spite of the considerable data available, a complete and unambiguous assignment of the chlorophyll *a* vibrational spectrum has not yet appeared. This is partly due to limitations imposed by the high fluorescence produced at many of the laser excitation wavelengths used to obtain RR spectra of chlorophylls. The use of metal-substituted chlorins and chlorophylls does allow observation of fluorescence-free RR spectra. However, the metal has a significant perturbing effect on the vibrational spectrum as well as on the properties of the chlorophyll (e.g. ligation, aggregation, etc.). Another approach for surmounting the fluorescence problem is the use of CARS spectroscopy. Höxtermann et al.[19] reported resonance CARS spectra of Chl *a* excited with 694.3 nm. However, this technique is experimentally demanding, and a more straightforward method is needed to determine the RR spectrum of chlorophylls with excitation into the lowest energy $^1\pi-\pi^*$ states.

Surface-enhanced Raman scattering (SERS) spectroscopy offers considerable promise for obtaining a complete excitation spectrum of the chlorophylls. This technique has been demonstrated as an effective method for obtaining spectra of highly fluorescent molecules. The enhancement effect can increase Raman scattering intensity by 10^3–10^6-fold, and adsorption of molecules on the SERS-active metal surface results in fluorescence quenching.[12,20,21] In addition, the coupling of RR enhancement with surface enhancement (surface-enhanced resonance Raman scattering (SERRS)) results in an increase in scattering intensity by a factor of 10^3–10^5 over that observed under resonance or surface conditions alone.[12,21] Many publications have appeared in which attempts were made to determine the theoretical basis for surface enhancement. It is generally accepted that there are two major classes of enhancement mechanisms. Electromagnetic mechanisms attribute the SERS enhancement to increased local electric fields at the metal surface. The increased field strength is due to excitation of the collective oscillations of the conduction electrons (surface plasmons) at the metal surface.[22-24] Molecular or chemical mechanisms attribute the enhanced scattering to the formation of new excited states via charge transfer (ad-atom) or to the formation of a molecule–metal complex.[25,26]

In spite of an incomplete understanding of the mechanism, SERS (SERRS) has been used to determine vibrational information from a large number of biologically significant molecules.[27-29] There have also been a number of studies pertaining to the chlorophylls or chlorophyll derivatives. Uphaus et al.[30] obtained SERRS spectra with 457.9-nm excitation for Chl *a*, bacteriochlorophyll *a* and bacteriopheophytin *a* monolayers on silver islands films. Andersson et al.[31] reported a Q_y-excited SERRS spectrum of Chl *a* multilayers on a silver film. Recently, SERRS was applied to the elucidation of the Raman spectrum of copper chlorophyllin *a*, a chlorin derivative, which was adsorbed on colloidal silver or gold and excited within the blue and red regions of the electronic absorption spectrum.[12]

Previous SERRS studies of Chl *a* have demonstrated that it is possible to obtain spectra under various conditions. The present study is concerned with a detailed comparison between the RR and SERRS spectra of Chl *a* obtained under various conditions of excitation. The use of SERRS provides detailed and highly resolved spectra of Chl *a* adsorbed on a roughened silver electrode. The similarity between the RR and SERRS spectra supports an electromagnetic mechanism as the dominant mode of enhancement at the silver surface and also demonstrates that structural alteration of chlorophyll *a* does not occur at a result of adsorption on the electrode surface. Each excitation wavelength produces a distinctive spectrum, indicating dramatic changes in mode enhancements. These intensity changes provide insights regarding the structural changes accompanying electronic excitation. The

(5) (a) Ozaki, Y.; Kitagawa, T.; Ogoshi, H. *Inorg. Chem.* **1979**, *18*, 1772–1776. (b) Ozaki, Y.; Iriyama, K.; Ogoshi, H.; Ochiai, T.; Kitagawa, T. *J. Phys. Chem.* **1986**, *90*, 6105–6112. (c) Ozaki, Y.; Iriyama, K.; Ogoshi, H.; Ochiai, T.; Kitagawa, T. *Ibid.* **1986**, *90*, 6113–6118.
(6) Ching, Y.; Ondrias, M. R.; Rousseau, D. L.; Muhoberac, B. B.; Wharton, D. C. *FEBS Lett.* **1982**, *138*, 239–244.
(7) (a) Andersson, L. A.; Loehr, T. M.; Lim, A. R.; Mauk, A. G. *J. Biol. Chem.* **1984**, *259*, 15340–15349. (b) Andersson, L. A.; Loehr, T. M.; Chang, C. K.; Mauk, A. G. *J. Am. Chem. Soc.* **1985**, *107*, 182–191. (c) Andersson, L. A.; Lochr, T. M.; Sotiriou, C.; Wu, W.; Chang, C. K. *J. Am. Chem. Soc.* **1986**, *108*, 2908–2916. (d) Andersson, L. A.; Sotiriou, C.; Chang, C. K.; Loehr, T. M. *J. Am. Chem. Soc.* **1987**, *109*, 258–264.
(8) (a) Cotton, T. M.; Timkovich, R.; Cork, M. S. *FEBS Lett.* **1981**, *133*, 39–44. (b) Cotton, T. M.; Van Duyne, R. P. *J. Am. Chem. Soc.* **1981**, *103*, 6020–6026. (c) Cotton, T. M.; Parks, K. D.; Van Duyne, R. P. *J. Am. Chem. Soc.* **1980**, *102*, 6399–6407.
(9) (a) Fujiwara, M.; Tasumi, M. *J. Phys. Chem.* **1986**, *90*, 250–255. (b) Fujiwara, M.; Tasumi, M. *Ibid.* **1986**, *90*, 5646–5650.
(10) (a) Lutz, M. In *Advances in Infrared and Raman Spectroscopy*; Clark, R. J. H., Hester, R. E., Eds.; John Wiley & Sons: New York, 1984; Vol. 11, pp 211–300. (b) Robert, B.; Lutz, M. *Biochemistry* **1986**, *25*, 2303–2309. (c) Lutz, M.; Hoff, A. L.; Brehamet, L. *Biochim. Biophys. Acta* **1982**, *679*, 331–341. (d) Lutz, M. *J. Raman Spectrosc.* **1974**, *2*, 497–516. (e) Lutz, M.; Breton, J. *Biochem. Biophys. Res. Commun.* **1973**, *53*, 413–418.
(11) Heald, R. L.; Callahan, P. M.; Cotton, T. M. *J. Phys. Chem.* **1988**, *92*, 4820–4824.
(12) Hildebrandt, P.; Spiro, T. G. *J. Phys. Chem.* **1988**, *92*, 3355–3360.
(13) (a) Boldt, N. J.; Donohoe, R. J.; Birge, R. R.; Bocian, D. F. *J. Am. Chem. Soc.* **1987**, *109*, 2284–2298. (b) Donohoe, R. J.; Atamian, M.; Bocian, D. F. *J. Phys. Chem.* **1989**, *93*, 2244–2252.
(14) Mattioli, T. A.; Haley, L. V.; Koningstein, J. A. *Chem. Phys.* **1990**, *140*, 317–329.
(15) Fonda, H. N.; Babcock, G. T. In *Progress in Photosynthesis Research*; Biggens, J., Ed.; Martinus Nijhoff: Boston, 1987; Vol. I, pp 449–452.
(16) Cotton, T. M.; Loach, P. A.; Katz, J. J.; Ballschmiter, K. *Photochem. Photobiol.* **1978**, *27*, 735–749.
(17) Lutz, M.; Kleo, J.; Gilet, R.; Henry, M.; Plus, R.; Leicknam, J. P. In *Proceedings of the 2nd International Conference on Stable Isotopes*; Klein, E. R., Klein, P. D., Eds.; U.S. Department of Commerce: Springfield, VA, 1975; pp 462–469.
(18) Nabedryk, E.; Leonard, M.; Mantele, W.; Breton, J. *Biochemistry* **1990**, *29*, 3242–3247.
(19) Höxtermann, B.; Wernicke, W.; Tscho, J. T.; Lau, A.; Hoffmann, P. *Studia Biophys.* **1986**, *115*, 85–94.
(20) Weitz, D. A.; Garoff, S.; Gersten, J. I.; Nitzan, A. *J. Chem. Phys.* **1983**, *78*, 5324–5338.
(21) Cotton, T. M.; Schultz, S. G.; Van Duyne, R. P. *J. Am. Chem. Soc.* **1980**, *102*, 7960–7962.
(22) Gersten, J. I.; Nitzan, A. *J. Chem. Phys.* **1980**, *73*, 3023–3037.
(23) Kerker, M.; Wang, D. S.; Chew, H. *Appl. Opt.* **1980**, *19*, 4159–4174.
(24) Ferrell, T. L. *Phys. Rev. B: Condens. Matter* **1982**, *25*, 2930–2932.
(25) Furtak, T. E. *J. Electroanal. Chem. Interfacial Electrochem.* **1983**, *150*, 375.
(26) Otto, A. In *Light Scattering in Solids*; Cardona, M., Gunthrodt, G., Eds.; Springer-Verlag: Berlin, 1984; Vol. IV, pp 289–461.
(27) Cotton, T. M. In *Spectroscopy of Surfaces*; Clark, R. J. H., Hester, R. E., Eds.; John Wiley & Sons: New York, 1988; Vol. 16, pp 91–153.
(28) Koglin, E.; Sequaris, J.-M. In *Topics in Current Chemistry*; Springer-Verlag: Berlin, 1986; Vol. 134, pp 1–53.
(29) Nabiev, I.; Efremov, R. G.; Chumanov, G. D. *Sov. Phys. Usp.* **1988**, *31*, 241–262.
(30) Uphaus, R. A.; Cotton, T. M.; Möbius, D. *Thin Solid Films* **1986**, *132*, 173–185.
(31) Andersson, L. A.; Loehr, T. M.; Cotton, T. M.; Simpson, D. J.; Smith, K. M. *Biochim. Biophys. Acta* **1989**, *974*, 163–179.

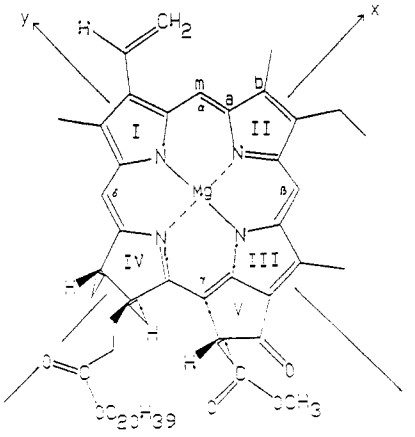

Figure 1. Structural diagram of chlorophyll *a*.

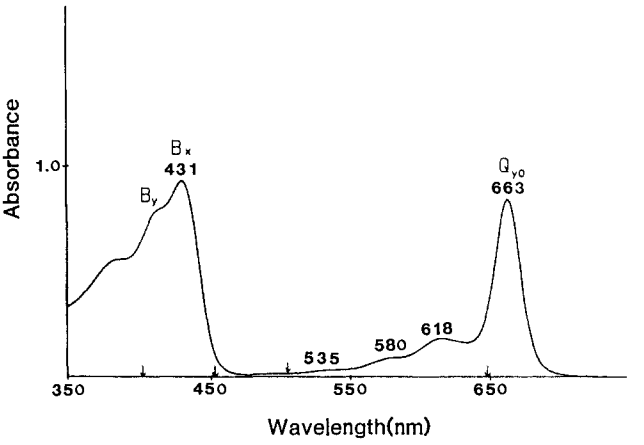

Figure 2. Absorption spectrum of Chl *a* in ACN–MeOH (3:1 v/v).

SERRS data also provide additional criteria for band assignments and suggest the mode of interaction of Chl *a* with the surface. Because the purpose of this study is to compare the RR and SERRS spectra of Chl *a*, a detailed discussion of each band assignment will not be given here. Rather, the analysis will be limited to those bands that are most affected by the interaction of Chl *a* with the silver surface.

Experimental Section

Chlorophyll *a* Preparation. Chl *a* (Figure 1) was isolated from spinach according to an established procedure.[32] Prior to use, the Chl *a* was purified by isocratic semipreparative reverse-phase high-performance liquid chromatography (rp HPLC) on a Phenomenex C18 guard column and Phenomenex 10 μm C18 25 cm × 10 mm i.d. column. The mobile phase was acetonitrile–methanol 3:1 (v/v) with a flow rate of 5 mL/min. All solvents were Omnisolv HPLC grade and were degassed prior to use by vacuum filtration. The HPLC equipment consists of a Model 2350 ISCO high-pressure pump, a Model 2360 ISCO gradient programer, and a Model V4 ISCO absorbance detector set at 445 nm. One milliliter of a Chl *a* solution in the mobile phase was injected into the system and the central portion of the Chl *a* peak was collected. The concentration of the eluent was typically ca. 2×10^{-4} M on the basis of its electronic absorption spectrum.

For RR experiments the purified Chl *a* solutions were placed in 5 mm o.d. Pyrex tubes, vacuum degassed with 3 freeze–pump–thaw cycles, and sealed under vacuum. For SERRS experiments the roughened electrode was immersed in the chosen chlorophyll fraction separated by HPLC. The Chl *a* was adsorbed onto the electrochemically roughened electrode by allowing the electrode to remain in the purified Chl *a* solution (2×10^{-4} M) for 10 min in the dark. The Chl *a* concentration on the electrode surface, approximately monolayer level (1×10^{-10} mol of Chl *a*/cm^2), was estimated by sonicating the electrode in CH_2Cl_2 and recording a fluorescence spectrum of the resulting solution. The electrode surface area was determined electrochemically to be 0.28 cm^2.

The purity of the Chl *a* was monitored and confirmed before and after the Raman experiments by analytical rp HPLC and UV–vis spectroscopy. A Phenomenex Ultrex 3 μm C18 7.5 cm × 4.6 mm i.d. column was used for the chromatography. Electronic absorption spectra were measured with use of a 1 cm pathlength cuvette and a Shimadzu J-260 UV–vis spectrophotometer.

Electrode Preparation. A silver electrode was used as the SERRS substrate. It was constructed by sealing a flattened silver wire into a glass tube with Torr seal. The exposed surface was rectangular with dimensions approximately 4 × 7 mm. The electrode was polished with use of successively finer grades of alumina (5.0, 0.3, 0.05 μm). The electrode was rinsed and sonicated between polishing steps. Following the polishing procedure the electrode was cleaned by cathodization at −2.0 V for 1 min and roughened by using an oxidation–reduction cycle (ORC) consisting of a double-potential step from an initial potential of −550 mV to +550 mV and back to −550 mV in 0.1 M Na_2SO_4 solution. The total charge passed during the oxidation step was equivalent to 25 mC/cm^2. A SSCE (saturated sodium calomel electrode) was used as the reference electrode and a Pt wire served as the auxiliary electrode.

Resonance Raman and SERRS Spectroscopy. Laser excitation of the Raman and surface Raman scattering was provided by a Coherent Innova 90 Ar^+ laser (457.9 and 514.5 nm) or a Coherent Innova 100 Kr^+ laser (406.7 and 647.1 nm). The laser power was 25 mW for all the spectra reported here. Raman scattered light was collected in a backscattering geometry.

SERRS spectra obtained with 647.1-nm excitation were recorded with a Spex Triplemate spectrometer coupled to a Princeton Applied Research Corp. (PARC) Model 1421-R-1024HD intensified SiPD detector cooled to −40 °C. The spectra were collected and processed with an OMA-3 (PARC) optical multichannel analyzer. RR and SERRS spectra obtained by excitation at the other wavelengths were recorded with a Model 1420 (PARC) intensified SiPD detector. These spectra were collected and processed with an OMA-2 (PARC) optical multichannel analyzer. The reported spectra are composites of 16 scans, with 5 and 1 s integration periods per scan for the RR and SERRS spectra, respectively.

SERRS spectra of the adsorbed Chl *a* at room temperature (298 K) were obtained by transferring the electrode to a quartz Dewar flask containing degassed HPLC grade water. The Dewar flask was constructed with a transparent body to allow direct acquisition of a SERRS spectrum during electrode immersion in water. Low-temperature (77 K) SERRS spectra of the adsorbed Chl *a* were obtained by transferring the electrode to the quartz Dewar flask containing liquid nitrogen.

Results

Electronic Absorption Spectroscopy. The electronic absorption spectrum of Chl *a*, together with several assigned transitions, is shown in Figure 2. The splitting is much greater between the Q_x and the Q_y transitions than between the B_x and B_y bands. This was originally observed in metallochlorins.[13a,33] In the Soret region of the spectrum, the B_x transition is strongest and occurs at 431 nm. The B_y transition is present as a blue shoulder at ca. 413 nm. In the green to red region of the spectrum, the four maxima at 663, 618, 580, and 535 nm are assigned as vibronic bands belonging to the Q_y and Q_x transitions. Until recently these bands were assigned as $Q_y(0,0)$, $Q_y(1,0)$, $(Q_x(0,0) + Q_y(2,0))$, and $Q_x(1,0)$, respectively.[34-36] There is still agreement that the 663-nm band is $Q_y(0,0)$. However, according to the linear dichroism and fluorescence polarization studies of Fragata et al.,[37] the 618-, 580-, and 535-nm vibronic bands belong to $Q_x(0,0)$, $(Q_y(1,0) + Q_x(1,0))$, and $(Q_x(0,0) + Q_y(2,0))$, respectively. The Q_x contribution to the 535-nm band is twice that of Q_y and, therefore, this band can still be considered to arise predominantly from an *x*-polarized electronic transition.

Raman Spectroscopy. The excitation wavelengths used for obtaining RR and SERRS spectra are given in the figure legends and indicated in Figure 2. Table I lists the major RR and SERRS (298 and 77 K) bands and their vibrational assignments. These

(32) Strain, H. H.; Svec, W. A. In *The Chlorophylls*; Vernon, L. P., Seely, G. R., Eds.; Academic: New York, 1966; pp 21–66.

(33) Weiss, C. In *The Porphyrins*; Dolphin, D., Ed.; Academic: New York, 1978; Vol. III, p 216.

(34) Weiss, C. *J. Mol. Spectrosc.* **1972**, *44*, 37–80.

(35) Petke, J. D.; Maggiora, G. M.; Shipman, L.; Christofferson, R. E. *Photochem. Photobiol.* **1979**, *30*, 203–223.

(36) Shipman, L. L.; Cotton, T. M.; Norris, J. R.; Katz, J. J. *J. Am. Chem. Soc.* **1976**, *98*, 8222–8230.

(37) Fragata, M.; Nordén, B.; Kurucsev, T. *Photochem. Photobiol.* **1988**, *47*, 133–143.

Table 1. Chl *a* RR and SERRS Frequencies (cm^{-1})

RR		SERRS[a]				
406.7[b]	457.9[b]	406.7[b]	457.9[b]	514.5[b]	647.1[b]	assignment[c]
1684		1677				$\nu C_9{=}O$
		1684				
1599	1599	1604	1611	1608		$\nu C_aC_m(\alpha,\beta)$
		1606	1610	1610	1602	
1548	1548	1550	1556	1554		νC_aC_b(III); νC_bC_b(I)
		1553	1555	1557	1538	
	1520	1535	1528	1528		νC_bC_b(I); νC_aC_b(III)
		1535	1529	1530		
1488		1490		1493		$\nu C_aC_m(\delta)$; νC_aC_b(I)
		1494	1490	1496	1490	
1433	1433	1429	1433	1444		$\nu C_aC_m(\gamma,\delta)$; νC_aC_b(I–III)
		1437	1437	1437	1429	
			1385	1390		νC_aC_b(II); $\nu C_aC_m(\alpha,\delta)$
			1385	1389	1385	
1379	1376	1377	1377	1376		νC_aN(IV); νC_aC_b(I,III)
		1379	1377	1376		
1344	1343	1350	1348	1346		νC_aN(IV); νC_aN(I,III)
		1357	1351	1346	1350	
		1329	1330	1327	1321	νC_aN(I); $\delta C_mH(\delta)$
		1329	1330	1328	1327	
1285	1290	1286	1287	1286	1285	$\delta C_mH(\alpha,\beta)$; νC_aN(II,IV)
		1288	1287	1288	1282	
					1262	
1221		1221		1231	1221	γC_bH(IV); $\delta C_mH(\delta)$
		1227		1231	1218	
	1210		1209	1216		γC_bH(IV); $\delta C_mH(\delta)$
			1208	1210		
1182	1182	1181	1184	1184	1180	νC_mC_{10}(V); δC_bH(IV)
		1186	1186	1186	1185	
1147	1150	1141	1146	1153	1139	νC_aN(II); δC_aNC_a(I)
		1144	1146	1159	1143	
		1072			1070	
	1042		1045			νC_aN(III)
		1050	1042	1046	1050	
986	988	987	984	982	981	νC_mC_aN(III); νC_9C_{10}(V)
		986	978	985	986	
914		914	918	918	911	δC_aC_bEt
		914	914	920	919	
791	796	794	795	795		δC_aC_bEt
		793	794	796	798	
751		751			743	δC_aC_bEt
		752	743	748	748	
	717	707	709	728		
		717	717			
686	698	698		695	694	
		696	703	700		
			577			
			577		569	
	513		498			
			519		519	
			464			
			467			
			344			
			344			
316	314					
			320			
253			265			
			274			
			213			
			184			

[a] The top frequency is at 298 K and the bottom frequency is at 77 K. [b] Excitation wavelength in nm. [c] Assignments based on those reported by Lutz,[10a] Hildebrandt et al.,[12] and Boldt et al.[13a] Mode descriptions are ν = stretch, δ = in-plane deformation, and γ = out-of-plane deformation. C_a, C_b, C_m and the characters in parentheses refer to the macrocycle positions shown in Figure 1.

assignments are based primarily on the recent normal mode analysis by Boldt et al.[13a]

High- and low-frequency RR spectra obtained with excitation in the B absorption band are shown in Figures 3 and 4, respec-

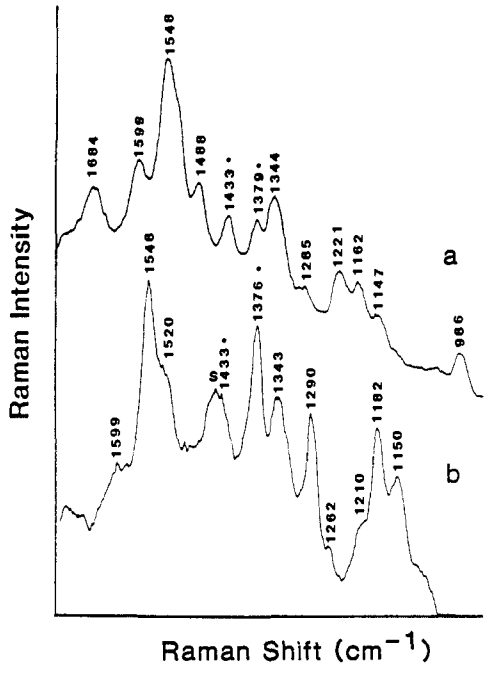

Figure 3. High-frequency RR spectra of 1.6×10^{-4} M Chl *a* in ACN-MeOH (3:1 v/v): laser power 25 mW; acquisition time 80 s; excitation wavelength (a) 406.7 nm and (b) 457.9 nm.

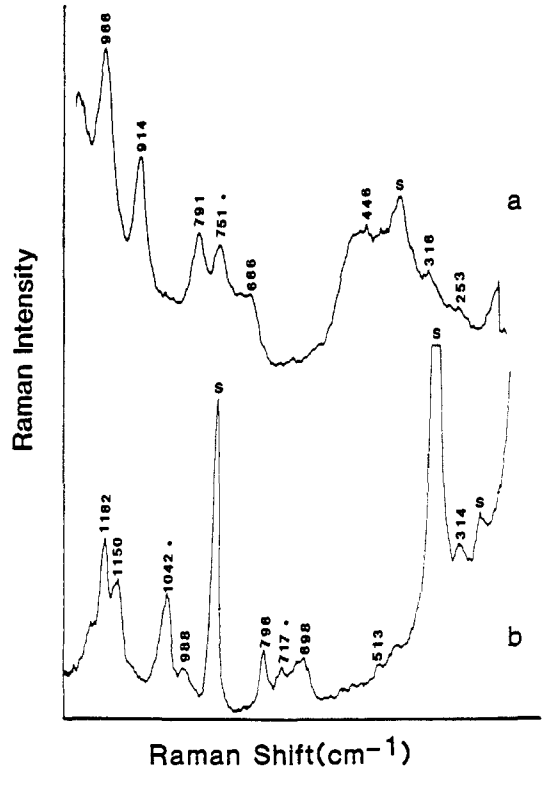

Figure 4. Low-frequency RR spectra of 1.6×10^{-4} M Chl *a* in ACN-MeOH (3:1 v/v). The experimental conditions are the same as in Figure 3.

tively. Figures 3a and 4a depict the spectra resulting from 406.7-nm excitation or in resonance with the B_y transition. Figures 3b and 4b show spectra of Chl *a* obtained with 457.9-nm excitation or in resonance with the B_x transition. The RR spectra are similar to those reported previously and are consistent with Franck-Condon activity of in-plane ring modes in resonance with the strongly allowed B transitions.[9a,10a,d,e,11] A comparison of the two spectra indicates strong bands at 1548 cm^{-1} (νC_aC_b(III); νC_bC_b(I)) at both excitation wavelengths. The 406.7-nm excited spectrum includes bands at 1684 ($\nu C_9{=}O$), 1599 ($\nu C_aC_m(\alpha,\beta)$), 1488 ($\nu C_aC_m(\delta)$; νC_aC_b(I)), and 1221 cm^{-1} (γC_bH(IV); $\delta C_mH(\delta)$); these bands are weak or absent in the 457.9-nm excited spectrum. This is reasonable considering that 406.7-nm light produces electronic excitation along the *y* axis of Chl *a* (Figure 1); the $C_9{=}O$ bond and ring I and ring III C_aC_b bonds lie parallel, or nearly so, to this axis. Modes containing bonds that are parallel to the electronic transition dipole moment and that are distorted in the excited state are expected to undergo the strongest enhancement. This does not explain the weak enhancement of the $\nu C_aC_m(\alpha,\beta,\delta)$ bands with 457.9-nm excitation, however. Previously, Lutz[10a] reported a medium-intensity 1599-cm^{-1} band and a very weak 1488-cm^{-1} band using 441.6-nm excitation. Perhaps 457.9 nm is too far removed from the B_x maximum for resonance enhancement of these modes. In contrast, bands at 1290 (δC_mH-(α,β); νC_aN(II,IV)), 1182 (νC_mC_{10}; γC_bH(IV)), and 1150 cm^{-1} (νC_aN(II); δC_aNC_a(I)) are more intense in the 457.9-nm excited spectrum as compared to their intensities in the 406.7-nm excited spectrum. This also appears acceptable because rings II and IV are aligned along the *x* axis and modes associated with these rings should be enhanced with laser lines close to the B_x transition. While both the B_x and B_y show strong enhancement of the C_aC_b and C_bC_b modes it appears the 457.9-nm portion of the B_x enhances pyrrole modes associated with the inner bonds of the macrocycle (νC_aN) and the B_y enhances pyrrole modes associated with the periphery of the macrocycle (νC_aC_m). The appearance of the MgN_4 bands with 457.9-nm excitation is also supportive of this inner selectivity. Within the 750–1100-cm^{-1} region, the spectra obtained at the two excitation wavelengths have more similarities than spectra in the high-frequency region. Some differences exist in the 400–750-cm^{-1} region, but this region has not been previously assigned and will not be discussed here.

Attempts to obtain Raman spectra with 514.5- and 568.2-nm excitation were unsuccessful with use of the solution concentrations employed here (2×10^{-4} M). These lines are not in resonance with the B bands and the Q_x transition is very weak. Fluorescence obscured the RR spectrum at the 647.1-nm excitation.

Figures 5 and 6 show Chl *a* high- and low-frequency SERRS spectra, respectively, obtained at room temperature (298 K) excited within the B and Q bands. The electrode was submerged in degassed water during spectral acquisition, and this appears to stabilize Chl *a* by dissipating sample heating and reducing photooxidation. Thus, the SERRS signals did not degrade during the time required to accumulate 16 scans. High- and low-frequency SERRS spectra of Chl *a* with excitation in the B and Q bands at 77 K are shown in Figures 7 and 8, respectively.

Discussion

Comparison of the RR vs SERRS Spectra. The use of B band excitation allows direct comparison of RR (Figures 3 and 4) and SERRS (Figures 5a,b and 6a,b) spectra. As can be seen the SERRS spectra are clearly surface enhanced and display sharper, better resolved peaks in spite of the fact that the absolute amount of Chl *a* present in the laser beam is ca. 10^7 lower than in the RR experiments. The RR spectra contain solvent bands, as indicated with an "S". The bands marked with an asterisk have contributions from both the solvent and Chl *a*. In contrast, intense SERRS spectra are observed with only very weak contributions from the solvent. This is a consequence of the much stronger interaction between Chl *a* and the Ag surface as compared to the solvent–Ag surface interaction, as well as to the additional resonance contribution to the Chl *a* surface spectrum. Overall, more peaks are observed in the low-frequency SERRS spectra as compared to the low-frequency RR spectra, especially with 457.9-nm excitation.

A similar, though not identical, intensity pattern is also noted on comparing the RR (Figures 3 and 4) and SERRS spectra (Figures 5a,b and 6a,b). The similarity of the RR and SERRS frequencies is indicative of an electromagnetic enhancement mechanism.[22-24,26,38] Chemical enhancement mechanisms result in frequency shifts as well as relative intensity changes in the

(38) Otto, A. *Appl. Surf. Sci.* **1980**, *6*, 309–355.

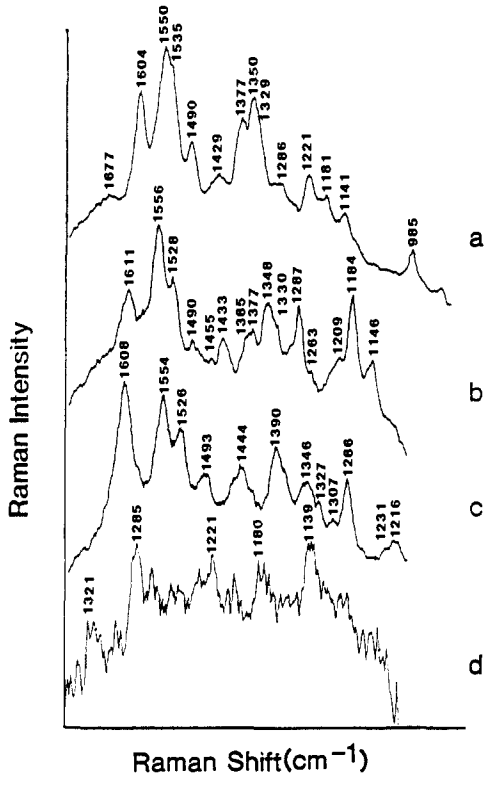

Figure 5. High-frequency SERRS spectra of Chl *a* adsorbed on a Ag electrode in degassed water: laser power 25 mW; acquisition time 16 s; 298 K; excitation wavelength (a) 406.7, (b) 457.9, (c) 514.5, and (d) 647.1 nm.

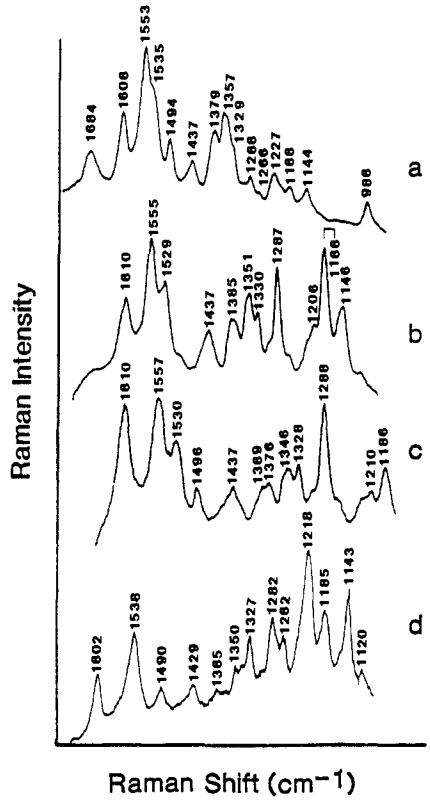

Figure 7. High-frequency SERRS spectra of Chl *a* adsorbed on a Ag electrode: laser power 25 mW; acquisition time 80 s; 77 K; excitation wavelength (a) 406.7, (b) 457.9, (c) 514.5, and (d) 647.1 nm.

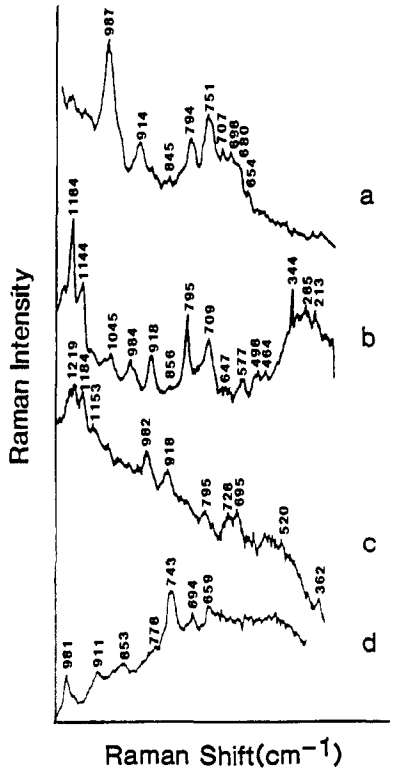

Figure 6. Low-frequency SERRS spectra of Chl *a* adsorbed on a Ag electrode in degassed water. The experimental conditions are the same as in Figure 5.

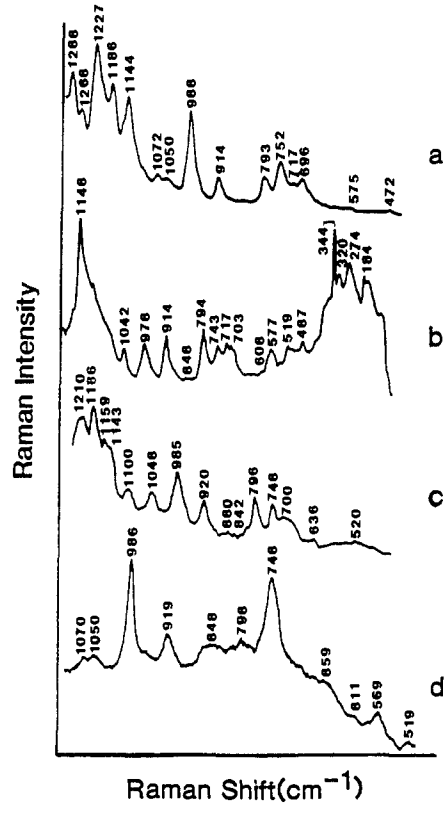

Figure 8. Low-frequency SERRS spectra of Chl *a* adsorbed on a Ag electrode. The experimental conditions are the same as in Figure 7.

SERRS spectra as compared to the RR spectra.[38] Also, the presence of peaks at 344 and 213 cm^{-1} (MgN_4 vibrations) indicates Chl *a* does not undergo detectable structural alterations upon adsorption.

Some differences do exist in frequencies and relative intensities of the bands, however. There are at least two possible origins for these differences. First, environmental effects may change the coordination state of Chl *a*. The solution spectra were recorded in acetonitrile–methanol (3:1) and the frequencies of coordination-sensitive bands are near those characteristic of six-coordinate Chl *a*.[9a] The surface spectra, on the other hand, are closer to

Table II. Comparison of RR and SERRS Bands (406.7- and 457.9-nm Excitation)

RR, cm^{-1}	Δ,[d] cm^{-1} 406.7 nm	457.9 nm	Δ[d] inten	assignment[a]
1599	+7	+11	>	$\nu C_aC_m(\alpha,\beta)$
1548	+5	+8	>	$\nu C_aC_b(III)$; $\nu C_bC_b(I)$
1520	*b*	+9	>	$\nu C_bC_b(I)$; $\nu C_aC_b(III)$
1488	+6	*b*	>>	$\nu C_aC_m(\delta)$; $\nu C_aC_b(I)$
1385	*b*	*b*	>	$\nu C_aC_b(II)$; $\nu C_aC_m(\alpha,\delta)$
1379	0	split	*c*	$\nu C_aN(IV)$; $\nu C_aC_b(I,III)$
1344	+13	+8, split	*c*	$\nu C_aN(I,III)$; $\nu C_aN(IV)$
1330	*b*	*b*	>	$\nu C_aN(I)$; $\delta C_mH(\delta)$
1290	+3	−3	0	$\delta C_mH(\alpha,\beta)$; $\nu C_aN(II,IV)$
1221	+6	*b*	0	$\gamma C_bH(IV)$; $\delta C_mH(\delta)$
1210	*b*	−2	0	$\gamma C_bH(IV)$; $\delta C_mH(\delta)$
1182	+4	+4	0	$\nu C_mC_{10}(V)$; $\gamma C_bH(IV)$
1147	−3	−4	0	$\nu C_aN(II)$; $\delta C_aNC_a(I)$

[a] See Table I and Figure 1 for references, abbreviations, and mode descriptions. [b] Peak does not appear in RR spectrum. [c] A portion of the frequency shift and decrease in intensity is due to the decrease in contribution by the solvent. [d] Δ (cm^{-1}) and Δ intensity = SERRS (77 K) value − RR value.

five-coordinate Chl *a*. Thus, a change in coordination may result following emersion of the electrode from the adsorbing solution. Second, relative intensity differences may reflect the orientation of the macrocycle at the metal surface. Electromagnetic enhancement theory attributes the relationship between band intensities and molecular orientation to the coupling of the electric field at the electrode surface with the polarizability tensors of the adsorbed molecule. Bonds that have polarizability tensors perpendicular to the electrode surface are preferentially enhanced.[39,40]

In order to predict the orientation of the Chl *a* on the surface, it is necessary to consider the nature of the forces involved in the adsorbate–surface interaction. There are two types: polar forces involving the interaction of the porphyrin macrocycle with the surface, and nonpolar forces arising from the phytol tails. Assuming that the Ag surface is hydrophilic, Chl *a* would be expected to interact through a polar functionality. There are several possibilities including the keto and ester groups on rings V and IV. Another possibility is that the vinyl moiety on ring I could interact with the surface through the formation of a π complex with Ag. Consideration of the van der Waal's interactions between the phytol tails suggests that surface-adsorbed structures producing maximal contact between the hydrophobic tails of adsorbed Chl's should be favored. As a result of the balance of these two forces, the adsorption of Chl *a* is expected to resemble that of other amphiphilic species[41] and result in a self-assembled monolayer structure.

An examination of the SERRS bands undergoing the greatest changes in frequency and/or intensity can provide evidence for a particular orientation of Chl *a* at the surface. Table II lists such bands as observed for B_x and B_y excitation. Only the high-frequency region is considered because differences between the SERRS and RR spectra were greatest here. From an analysis of the data shown in Table II, it is doubtful that the chlorophyll macrocycle lies parallel to the plane of the Ag surface for three reasons. First, if Chl *a* were to adsorb flat on the Ag surface, the polarizability tensors involving stretching vibrations of the pyrrole rings would lie parallel to the surface and these modes should not be strongly enhanced. Yet, inspection of Table II shows that these ring modes (1599, 1548, 1520, 1343, 1330 cm^{-1}) are precisely the ones that experience the greatest change at the surface. Second, the out-of-plane modes in the low-frequency region should be enhanced with parallel orientation. However, the low-frequency SERRS spectra are not strongly enhanced relative to the RR spectra. Third, a parallel orientation of the macrocyclic plane is not possible because of steric hindrance by the substituents on ring IV and V.

On the basis of previous spectral studies of monolayers of Chl *a* and other surface-active porphyrins, it is highly probable that the Chl *a* macrocycle is adsorbed at some angle to the Ag surface. Bocian et al.,[41] in a RR study of monolayer assemblies of Zn(II)-, Cu(II)-, and Co(II)-substituted H_2TOOP [5,10,15,20-tetrakis-[4-(1-octyloxy)phenyl]porphyrins] on glass slides, determined that the porphyrin planes were tilted at an angle of ca. 40°; the planes were 4–5 Å apart and canted at an angle of approximately 47° with respect to one another.

Considering next the likely site of molecule–surface interaction, it is expected that if Chl *a* adsorption occurred through any of the substituents on rings IV or V, the carbonyl vibrations (ester or ketone) should be observed in the SERRS spectra. Enhancement of these modes is to be expected because of proximity of the oxygen functionalities to the surface and also because a component of the polarizability tensor would lie perpendicular to the surface. However, a significant enhancement of the C=O modes is not observed in the SERRS spectra and it is concluded that these groups are not strongly interacting with the surface. A shift and broadening of the C-9 keto group from 1684 (Figure 3) to 1677 cm^{-1} (Figure 5) is observed in the 406.7-nm spectrum, which may reflect a weak interaction of this group with the surface.

Soriaga and Hubbard[42] have reported that aromatic molecules adsorbed on smooth platinum electrodes reorient to form structures occupying a minimal surface area. This suggests that adsorption of Chl *a* at only one ring contact is favored over a structure requiring contact of two rings with the surface. Another feature of the interaction of only a single ring with the surface is that this arrangement would favor maximum contact between the phytyl tails, i.e., the projection of the macrocycle at the surface is minimal, providing closest packing of the tails.

Although an edge-on orientation of the Chl *a* macrocycle is clearly supported by the SERRS spectra, it is premature to speculate as to which edge is nearest the surface. It is conceivable that there are a number of orientations that result from spontaneous adsorption. Langmuir–Blodgett techniques will be used in future SERRS studies of the chlorophylls in an effort to control orientation.

Figures 5c,d and 6c,d are SERRS spectra of Chl *a* at 298 K with 514.5- and 647.1-nm excitation, respectively. Resonance Raman spectra could not be obtained at these excitation wavelengths. With use of 514.5-nm excitation, the RR scattering was very weak at the solution concentration employed. Excitation at 647.1 nm resulted in intense fluorescence which obscured the RR spectrum. Overall, the SERRS technique provides several major advantages for spectroscopic studies of Chl *a*. These advantages include extremely high sensitivity, fluorescence quenching, and improved spectral resolution for all excitation wavelengths used in this study.

Nonetheless, the Ag surface did not completely quench fluorescence when 647.1-nm excitation was used (Figures 5d and 6d) at 298 K. In fact, in the region 1300–1700 cm^{-1} (not shown) the Raman peaks were indiscernible from the background. The fluorescence was much weaker in the low-frequency region of the spectrum, but the overall spectral intensity was not as great as that observed with B band excitation (Figures 5a,b and 6a,b).

Surface-Enhanced Resonance Raman Scattering at 77 K. To minimize sample photodegradation and fluorescence, SERRS spectra were recorded at liquid nitrogen temperature (Figures 7 and 8). In general, spectra recorded at this temperature showed a dramatic suppression of broad-band emission, with narrower peaks, and frequency shifts when compared with SERRS spectra at room temperature. The spectral differences between SERRS at 298 and 77 K were greatest with 406.7-nm excitation. As can be seen from the figures, the C_9=O mode is much stronger and is up-shifted to 1684 cm^{-1} in the low-temperature spectrum. This shift may be indicative of a change in orientation of the macrocycle

(39) Van Duyne, R. P. In *Chemical and Biochemical Applications of Lasers*; Moore, C. B., Ed.; Academic Press: New York, 1979; Vol. IV, p 101.
(40) Moskovits, M. *J. Chem. Phys.* **1982**, *77*, 4408–4416.
(41) Schick, G. A.; Schreiman, I. C.; Wagner, R. W.; Lindsey, J. S.; Bocian, D. F. *J. Am. Chem. Soc.* **1989**, *111*, 1344–1350.
(42) Soriaga, M. P.; Hubbard, A. T. *J. Am. Chem. Soc.* **1982**, *104*, 3937–3945.

with respect to the surface, a change in the electronic properties of the molecule with temperature, a conformational change in the macrocycle, or some combination of these three possibilities.

Figures 7 and 8 display SERRS spectra of Chl *a* at 77 K excited with various laser lines ranging from the violet to the red region of the electromagnetic spectrum. Changes in the spectra with excitation wavelength are more distinct than at 298 K. The excitation frequency dependent changes will be discussed below. Most significantly, at 77 K the fluorescence was quenched at the roughened Ag electrode and sample photooxidation was minimized, permitting acquisition of the entire spectrum. The remainder of the discussion will include only the SERRS results obtained at 77 K.

It is evident from Figures 7 and 8 that some bands that are strong at one excitation wavelength are not even observed at other excitation wavelengths. Differences in enhancement patterns are expected from a consideration of the differing enhancement mechanisms that are operative under B and Q excitation conditions, as described in the Introduction. The considerable variation in intensity patterns with changes in excitation wavelength was also noted in the RR studies of $ClFe^{III}$ pheophorbide by Andersson et al.[31] and in the SERRS studies of copper chlorophyllin with silver and gold colloid particles.[12] In the latter study it was concluded that the Ag particles do not significantly perturb the copper chlorophyllin electronic states. Similarly, the data shown here also indicate that the Ag electrode surface does not significantly perturb the Chl *a* electronic states.

Excitation within the B_y absorption band with use of the 406.7-nm line produces a spectrum dominated by totally symmetric Franck–Condon-active modes aligned along the *y* axis of the macrocycle. The spectrum obtained with 457.9-nm excitation is in resonance with the B_x absorption band, and modes composed of bonds aligned along the *x* axis of the macrocycle are preferentially enhanced.

A comparison of the 406.7- and 457.9-nm excited spectra shows that the 1494-cm^{-1} band in the former is absent and the 1535-cm^{-1} shoulder is clearly resolved and shifted to the 1529-cm^{-1} band with 457.9-nm excitation. Also, as previously discussed in the context of the RR spectra, modes in the 1300–1100-cm^{-1} range are strongly enhanced with B_x but not with B_y excitation. The νC_aN bands in the 1300–1400-cm^{-1} region are more highly resolved in the 457.9-nm spectrum. The orientation of the macrocycle relative to the surface results in differing enhancements for the νC_aN of the various rings. The 1610-cm^{-1} band νC_aC_m that appears in the 457.9-nm SERRS spectrum is assigned to $C_aC_m(\alpha,\beta)$ modes. The low-frequency region of the B_x excited spectrum contains many more peaks than the B_y excited spectrum. The presence of the 320 and 184 cm^{-1} (MgN_4) bands in the 457.9-nm excited spectrum suggests this an appropriate wavelength for selective monitoring of these modes in the study of photosynthetic reaction centers.

An examination of the 514.5-nm excited spectrum shows that it is very similar to that observed with 457.9-nm excitation. The 514.5-nm wavelength is in resonance with a weak absorption band which has a major contribution from the $Q_x(0,0)$ transition.[37] Thus, it is expected that these spectra should be similar because both electronic transitions lie parallel to the *x* axis. Coupling between the B_x and Q_x transitions may additionally occur in the 514.5-nm spectrum. The 514.5-nm excited spectrum particularly resembles the 457.9-nm excited spectrum with regards to the splitting of the νC_aN modes and the presence of the 1528-cm^{-1} band. The 1385-cm^{-1} band of the latter spectrum is well-resolved from the other C_aN modes and is split into bands at 1389 and 1376 cm^{-1} in the 514.5-nm spectrum.

In addition, the B_x and Q_x excited spectra are similar in the low-frequency region. However, the peaks at 1186 and 1146 cm^{-1} are much stronger in the B_x than in the Q_x excited spectrum and the MgN_4 vibrations are not enhanced in the latter.

Red excitation within the Q_{y0} absorption band produces a spectrum that has some features in common with all of the other spectra but also presents some unique features. The region most enhanced is between 1250 and 1100 cm^{-1}, where the C–H bending vibrations are found. It has been proposed that the 1218- and 1185-cm^{-1} bands also contain contributions from out-of-plane C_bH modes.[13a] The 1100–1300-cm^{-1} region of the spectrum resembles spectra reported recently for Ni Pheo *a* as obtained with Q_y excitation.[14] The close correspondence between the spectra of these compounds in this region is reasonable because these modes are not metal sensitive.[10a] As with 457.9- and 514.5-nm light the splitting of the νC_aN modes occurs in the 1300–1400-cm^{-1} region. In the low-frequency region the Q_{y0} excited spectrum resembles the B_y excited spectrum in that both have a strong 986-cm^{-1} band ($\nu C_9C_{10}(V)$; δC_mC_aN). In contrast with the other spectra, only the Q_{y0} excited spectrum displays a strong 748-cm^{-1} band (δC_aC_bEt).

The Q_{y0} band is intense and, as noted previously, excitation within this transition results in both Franck–Condon scattering and vibronic activity.[12,14] Vibrational modes aligned along the *y* axis are expected to have the largest Franck–Condon overlap integrals. However, the bands enhanced with 406.7-nm (B_y) excitation are not the same as those enhanced with 647.1-nm (Q_{y0}) excitation. Among the wavelengths used in this study, only the 406.7-nm excited spectrum displays the peak assigned as $\nu C_9{=}O$ at 1684 cm^{-1}. Because the symmetric $C_9{=}O$ stretch is aligned along the *y* axis it is expected that this vibration should also appear in the Q_y spectrum, but this is not observed. This implies that the Franck–Condon active modes are different for the B_y and Q_{y0} transitions. Changes in the ground-state configuration with respect to the excited state are not the same for B_y and Q_{y0} excitation.

Conclusions

The spectra presented in this paper are the first SERRS spectra of Chl *a* obtained with laser excitation wavelengths ranging from the violet to the red region of the electromagnetic spectrum. Distinct SERRS spectra were observed for each excitation wavelength, and the enhancement pattern is typical of that reported previously for RR excitation of Chl *a* within the B electronic absorption bands, i.e. Franck–Condon scattering is the major source of enhancement resulting from excitation within the B bands and vibronic coupling mechanisms are dominant for excitation within the Q_x absorption band. A comparison of the RR and SERRS spectra at two excitation wavelengths within the B transitions shows clearly that adsorption of Chl *a* does not cause a significant perturbation of these two electronic states. Only minor frequency shifts are observed in the surface as compared to solution spectra. Thus, surface enhancement results primarily from an electromagnetic mechanism.

The intensity differences between the SERRS and RR spectra may reflect both environmental effects as well as orientation of the macrocycle with respect to the surface. Surface-selection rules predicted by electromagnetic theory can be used to determine orientation. Future studies will include the characterization of Langmuir–Blodgett monolayers of Chl *a* at a metal surface. This technique will allow better experimental control over Chl *a* orientation.

The spectra obtained in resonance with Q_y are of particular importance. Previously, it has not been possible to observe RR scattering from Chl *a* with excitation wavelengths in resonance with this state because of intense fluorescence emission. The fluorescence-quenching advantage of SERRS makes it ideally suited for the objective of this study. A comparison of the SERRS spectrum of Chl *a* with the RR spectrum of Ni Pheo *a*[14] shows that the enhancement pattern is similar, especially in the 1200–1300-cm^{-1} region of the spectrum which is dominated by C–H bending modes and is relatively insensitive to the central metal ion. This fact, together with the similarity between the SERRS and RR spectra at the blue and green excitation wavelengths, lends further credence to the use of SERRS as a method of choice for observing vibrational spectra of Chl *a* when excited within the Q_y transition. The SERRS spectrum provides unique insights regarding the electronic properties of this state, and this technique should be useful for obtaining resonance excitation profiles within the lowest energy transition.

Resonance Raman spectroscopy has been used extensively for the study of a variety of photosynthetic preparations,[43] as well

as for characterizing the isolated chlorophylls. The goal of these studies has been to provide structural information regarding the organization of the chlorophylls within the photosynthetic membrane. Such information elucidates the mechanistic role of these important pigments in the photosynthetic processes (i.e. light harvesting and electron-transfer steps). The results presented herein suggest that SERRS offers a viable approach for the study of intact photosynthetic preparations. Our previous studies of reaction centers[44] and chromatophore preparations[45] have already demonstrated that SERRS studies of designated membrane components are feasible. In addition to the fluorescence quenching advantage, SERRS provides extremely high sensitivity, thereby minimizing the amount of material required for spectral analysis. The distance sensitivity can be used to obtain information concerning the spatial relationship of various components to the membrane surface. Finally, the ability to control the potential at an electrode surface suggests that SERRS may also be useful for determining spectra at fixed redox states of the reaction center.

Acknowledgment. Ames laboratory is operated for the U.S. Department of Energy by Iowa State University under contract No. W-7405-Eng-82. This article was supported by the Division of Chemical Sciences, Office of Basic Energy Sciences.

(43) Lutz, M.; Robert, B. In *Spectroscopy of Biological Molecules*; Alix, A. J. P., Bernard, L., Manfait, M., Eds.; Wiley: New York, 1985; pp 310-318.

(44) Cotton, T. M.; Van Duyne, R. P. *FEBS Lett.* **1982**, *147*, 81-84.

(45) (a) Picorel, R.; Holt, R. E.; Cotton, T. M.; Seibert, M. In *Progress in Photosynthesis Research*; Biggins, J., Ed.; Martinus Nijhoff Publishers: The Netherlands, 1987; pp 1.4, 423-426. (b) Picorel, R.; Holt, R. E.; Cotton, T. M.; Seibert, M. *J. Biol. Chem.* **1988**, *263*, 4374-4380. (c) Seibert, M.; Cotton, T. M.; Metz, J. G. *Biochim. Biophys. Acta* **1988**, *934*, 235-246. (d) Picorel, R.; Lu, T.; Holt, R. E.; Cotton, T. M.; Seibert, M. *Biochemistry* **1990**, *29*, 707-712.

Communications to the Editor

Synthesis and X-ray Crystal Structure Determination of a Novel Chiral Heteropolyanion: The "3:1" Octadecatungstohexaphosphate[1]

Rafael Acerete* and Juan Server-Carrió

Departamento de Química Inorgánica, Facultad de Farmacia Universitat de València, Blasco Ibáñez 13. 46010 Valencia, Spain

Angel Vegas and Martín Martínez-Ripoll

U.E.I. de Cristalografía Instituto "Rocasolano" CSIC, Serrano 119, 28006 Madrid, Spain

Received July 2, 1990

Polyoxometalates[2] are well-known compounds, which over the past few years have received increasing attention, owed in part to the recognition of their potential in areas such as catalysis,[3] photochemistry,[4] and medicine,[5] among others. Polyoxotungstophosphates constitute by far the most *fertile*, rapidly expanding heteropoly system, which shows an amazing structural *diversity* not encountered in any other heteroatom system. Most polytungstophosphates characterized thus far are obtained from rather acidic solutions (pH <5) or result from their partial decomposition to *lacunary* derivatives or condensations[7] of these lacunary species at appropriate pH. Yet, the *bulk* of polytungstophosphates present in weakly acidic (pH 5-7) aqueous solutions of WO_4^{2-} and HPO_4^{2-} remain relatively unexplored, even though their existence was reported more than a century ago.[7,8]

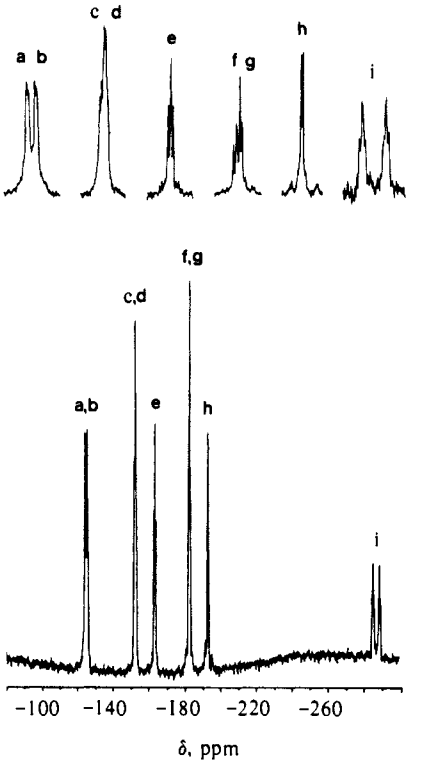

Figure 1. 200-MHz ^{183}W NMR spectrum of a 0.2 M solution of **1** (bottom) and expansion of peaks (top) in D_2O (61 104 transients). Chemical shifts (in ppm) are referenced to saturated Na_2WO_4/D_2O (substitution method) and negative to high field.

The heteropolyanions present in such nearly neutral solutions generally have a relatively high phosphorus content (W/P < 4). Two of them, namely, the $[P_4W_8O_{40}]^{12-}$ and $[P_4W_{14}O_{58}]^{12-}$ heteropolyanions,[9,10] have only recently been fully characterized. There are old reports[7b,8] on the existence of another phosphorus-rich heteropoly compound having a W/P ratio of 3:1, thus far formulated as $[(PW_3O_{13})_x]^{3x-}$, but to our knowledge, nothing

(1) From a portion of the Universitat de València Doctoral Dissertation of Juan Server-Carrió.

(2) (a) Pope, M. T. *Heteropoly and Isopoly Oxometalates*; Springer-Verlag: New York, 1983. (b) Pope, M. T. In *Comprehensive Coordination Chemistry*; Wilkinson, G., Gillard, R. D., McCleverty, J. A., Eds.; Pergamon: New York, 1987; Vol. 3, Chapter 38. (c) Weakley, T. J. R. *Struct. Bonding (Berlin)* **1974**, *18*, 131.

(3) Koshevnikov, I. V.; Matveev, K. I. *Russ. Chem. Rev. (Engl. Transl.)* **1982**, *51*, 1075. Matsuura, I.; Mizuno, S.; Hashiba, H. *Polyhedron* **1986**, *5*, 111. Hill, C. L.; Brown, R. B. *J. Am. Chem. Soc.* **1986**, *108*, 536.

(4) Papaconstantinou, E. *Chem. Soc. Rev.* **1989**, *18*, 1.

(5) (a) Jasmin, C.; Chermann, J. C.; Hervé, G.; Tézé, A.; Souchay, P.; Boy-Loustau, C.; Raybaud, N.; Sinoussi, F.; Raynaud, M. *J. Natl. Cancer Inst.* **1974**, *53*, 469. (b) Rozenbaum, W.; Dormont, D.; Spire, B.; Vilmer, E.; Gentillini, M.; Griscelli, C.; Montagnier, L.; Barre-Sinoussi, F.; Chermann, J. C. *Lancet* **1985**, 450.

(6) Contant, R.; Tézé, A. *Inorg. Chem.* **1985**, *24*, 4610.

(7) (a) Kehrmann, F. *Z. Anorg. Chem.* **1892**, *1*, 437. (b) Kehrmann, F.; Mellet, R. *Helv. Chim. Acta* **1922**, *5*, 942.

(8) (a) Souchay, P. *Ann. Chim. (Paris)* **1947**, *2*, 203. (b) Dubois, S.; Souchay, P. *Ann. Chim. (Paris)* **1948**, *3*, 105.

(9) Gatehouse, B. M.; Jozsa, A. J. *Acta Crystallogr., Sect. C: Cryst. Struct. Commun.* **1983**, *C39*, 658.

(10) Thouvenot, R.; Tézé, A.; Contant, R.; Hervé, G. *Inorg. Chem.* **1988**, *27*, 524.

0002-7863/90/1512-9386$02.50/0